Applied Catalysis B: Environmental 121–122 (2012) 206–213

Contents lists available at SciVerse ScienceDirect

Applied Catalysis B: Environmental

journal homepage: www.elsevier.com/locate/apcatb

Organic dye-sensitized TiO_2 as a versatile photocatalyst for solar hydrogen and environmental remediation

Sung Kyu Choi[a], Hyun Sik Yang[b], Jae Hong Kim[b], Hyunwoong Park[c,*]

[a] Department of Physics, Kyungpook National University, Daegu 702-701, Republic of Korea
[b] Department of Chemical Engineering, Yeungnam University, Gyeongsan 712-749, Republic of Korea
[c] School of Energy Engineering, Kyungpook National University, Daegu 702-701, Republic of Korea

ARTICLE INFO

Article history:
Received 18 January 2012
Received in revised form 4 April 2012
Accepted 8 April 2012
Available online 13 April 2012

Keywords:
Water splitting
Artificial photosynthesis
Dye structure
Cr reduction
Electron donors

ABSTRACT

This study explores the applicability of organic dye-sensitized TiO_2 particles in the production of molecular hydrogen and remediation of environmental pollutants (4-chlorophenol and Cr(VI)) under visible light ($\lambda > 420$ nm). In order to examine the effect of number of anchoring groups, Ru-free organic dyes of donor–π–acceptor configuration are prepared with different numbers (n) of carboxylate anchoring groups ($n = 1$, 2, and 3; referred to as D1, D2, and D3, respectively). All the three dyes are found to be effective at producing H_2 in the presence of electron donors (triethanolamine (TEOA) and ethylenediaminetetra-acetic acid (EDTA)) with the following orders: D3–D2 > D1 (TEOA) and D3 > D2–D1 (EDTA). FTIR studies reveal that D1 and D3 are anchored to the TiO_2 surface primarily via bidentate modes with a single carboxylate and two carboxylates, respectively. D2, in contrast, is anchored with one or two carboxylates, depending on the competing electron donors. The number of carboxylates is less important in the sensitized remediation of pollutants likely due to different photochemical conditions (oxic vs. anoxic) and various reaction pathways. A detailed systematic study is performed, including the UV–vis absorption characterization of free dyes and dye/TiO_2 samples, the photoelectrochemical behaviors of dye/TiO_2 electrodes, and the effects of dye concentrations, solution pH, and TiO_2 kind (Degussa P25 vs. Hombikat UV-100).

1. Introduction

Dye sensitization of TiO_2 is a promising and highly applicable process to generate electricity [1,2], produce renewable solar hydrogen [2–5], and remediate aqueous pollutants. In the sensitization process, dye molecules anchored to the TiO_2 surface are initially photo-excited and subsequently inject electrons to the TiO_2 conduction band. These electrons are then transported to interfacial electron acceptors (e.g., I_3^-, H_2O, H^+, dissolved O_2, and other substrates) and induce various redox reactions (Scheme 1) [2,5]. In this regard, enhanced light absorption and effective interfacial charge transfer from excited dye to TiO_2 should be the key parameters to attain a high level of photo-conversion efficiency [6–11].

A variety of sensitizers have been developed, among which Ru-bipyridyl complexes (Rubpy) are by far the most popular and display relatively high efficiency [1,2,6–10,12]. When Rubpy is used for H_2 production, the number and the kind of anchoring group are very critical. Not only these factors affect the optical properties of Rubpy, but the anchoring groups are also directly linked to the TiO_2 surface and thus work as an interfacial charge transfer channel [7,10]. There is still much debate as to the optimal number and position of carboxylates for Rubpy to be anchored to the TiO_2 surface effectively and robustly [7,9,13,14]. Despite such interesting phenomena, the high cost and environmental toxicity of Ru metal hinders its widespread application.

Recently, Ru-free organic sensitizers have been explored as an alternative to Rubpy in the dye-sensitized solar cells [15–21]. Typical organic sensitizers have D–π–A dipolar architectures, where a π-electron rich donor (D) is linked to a π-electron deficient acceptor (A) via a π bridge [19,22,23]. For effective anchoring, the acceptors are typically composed of carboxylate groups. Upon photoexcitation, intramolecular charge transfer from D to A occurs, and subsequently photogenerated electrons are injected into the TiO_2 conduction band. The overall photoefficiency of organic sensitizers highly depends on the number of anchoring groups, similar to the case in Rubpy. Interestingly, most organic sensitizers have only a single anchoring group despite having two more donor groups. This limits the robustness of coupling to TiO_2 [11,19,20,24]. In this regard, synthesis and use of multi-branched, multi-anchoring organic sensitizers is of great scientific interest and may lead to various applications.

* Corresponding author. Tel.: +82 53 950 7371.
E-mail address: hwp@knu.ac.kr (H. Park).

0926-3373/$ – see front matter © 2012 Elsevier B.V. All rights reserved.
http://dx.doi.org/10.1016/j.apcatb.2012.04.011

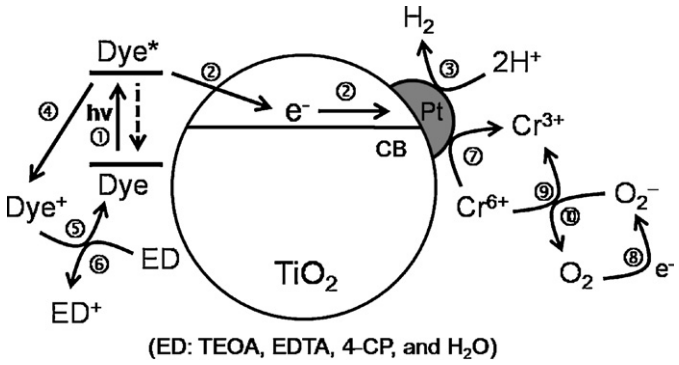

Scheme 1. Illustration of visible light induced H_2 production and remediation of environmental pollutants on organic dye-sensitized TiO_2 particles in water. 1: Photoexcitation and relaxation of dye, 2: electron injection to TiO_2 (or Pt/TiO_2) conduction band, 3: H_2 production, 4: oxidation of dye, 5: regeneration of dye, 6: oxidation of electron donors (ED), 7 and 9: reduction of Cr(VI) to Cr(III), 8: reduction of dissolved O_2 to superoxide anion, 10: oxidation of superoxide anion.

The aim and scope of this study is to compare tri-branched organic dyes with mono-, di-, and tri-carboxylate anchoring groups (sensitizers D1, D2, and D3, respectively: see Scheme 2) in terms of their solar hydrogen production in the presence of two well-known electron donors (TEOA vs. EDTA). Remediation of aqueous pollutants (4-chlorophenol and Cr(VI)) by the sensitized TiO_2 will also be explored. Upon testing of these sensitizers in the dye-sensitized solar cells with non-aqueous electrolytes, the overall cell efficiency has been reported to be 6.3% with D3, 6.1% with D2, and 4.9% with D1, while a reference sensitizer N3 has efficiency of 7.5% [25]. It is interesting to investigate whether such an efficiency order is still valid in H_2 production and remediation of pollutants in aqueous conditions because the charge transfer efficiency and stability of sensitizers should be significantly different between non-aqueous and aqueous environments. Surface analyses and electrochemical study of sensitized TiO_2 samples are also carried out to gain insight into the anchoring states of the sensitizers and the photo-induced electron transfers. To the best of our knowledge, there is no prior report on a systematic comparison of the effect of organic dye structures in an aqueous environment.

2. Experimental

2.1. Synthesis of dyes

The basic molecular structure of organic dyes involves a single donor, three acceptor groups, and a varying number of anchoring groups (Scheme 2). Each dye was synthesized through the Suzuki-coupling reaction, the Vilsmeire–Haack reaction, and the Knoevenagel condensation [21,25]. In brief, tris-(4-bromo-phenyl)-amine (**1**) that was synthesized from the reaction of triphenylamine and bromine was transformed into tris-(4-thiophene-phenyl)-amine (**2**) by the reaction with tributyl-thiophene-stannane in the presence of a Pd-complex. Then, **2** was reacted with $POCl_3$ in 1,2-dichloroethane solution in the presence of DMF with different concentrations of $POCl_3$ and DMF to obtain 4-[bis-(4-thiophene-phenyl)-amino]-phenyl-thiophene-2-carbaldehyde (**3**), 4,4′-[(4″-(thiophen-phenyl)]-bis-[thiophene-2-carbaldehyde] (**4**), and 5,5′,5″-(4,4′,4″-nitrilotris(benzene-4,1-diyl))trithiophene-2-carbaldehyde (**5**). For syntheses of D1, D2, and D3, the **3**, **4**, and **5**, respectively, were added to glacial acetic acid solution in the presence of 2-cyanoacetic acid and refluxed with ammonium acetate. The yields of D1, D2, and D3 were 79, 96, and 72%, respectively. Elemental analysis for D1 ($C_{34}H_{22}N_2O_2S_3$): Calculated: (%) C, 69.60; H, 3.78; N, 4.77; O, 5.45; S, 16.39. Found: (%) C, 68.90; H, 4.02; N, 4.22; S, 15.79. Elemental analysis for D2 ($C_{38}H_{23}N_3O_4S_3$): Calculated: (%) C, 66.94; H, 3.40; N, 6.16; O, 9.39; S, 14.11. Found: (%) C, 66.11; H, 3.48; N, 6.23; S, 14.59. Elemental analysis for D3 ($C_{42}H_{24}N_4O_6S_3$): Calculated: (%) C, 64.93; H, 3.11; N, 7.21; O, 12.36; S, 12.38. Found: (%) C, 64.24; H, 3.80; N, 7.89; S, 11.85.

2.2. Preparation and characterization of dye/TiO_2 samples

TiO_2 (Degussa P25), a mixture of anatase and rutile (8:2) with an average BET surface area of ca. 50 m^2/g was used as the main support of the dyes. Another commercial TiO_2 (Hombikat UV-100), an anatase with an average surface area of ca. 300 m^2/g was also employed as a support. To ensure effective hydrogen production, platinum nanoparticles were loaded onto TiO_2 particles using a photodeposition method [10]. Platinization was carried out by suspending TiO_2 particles in distilled water at 0.5 g/L in the presence of methanol (20 vol%) as an electron donor and

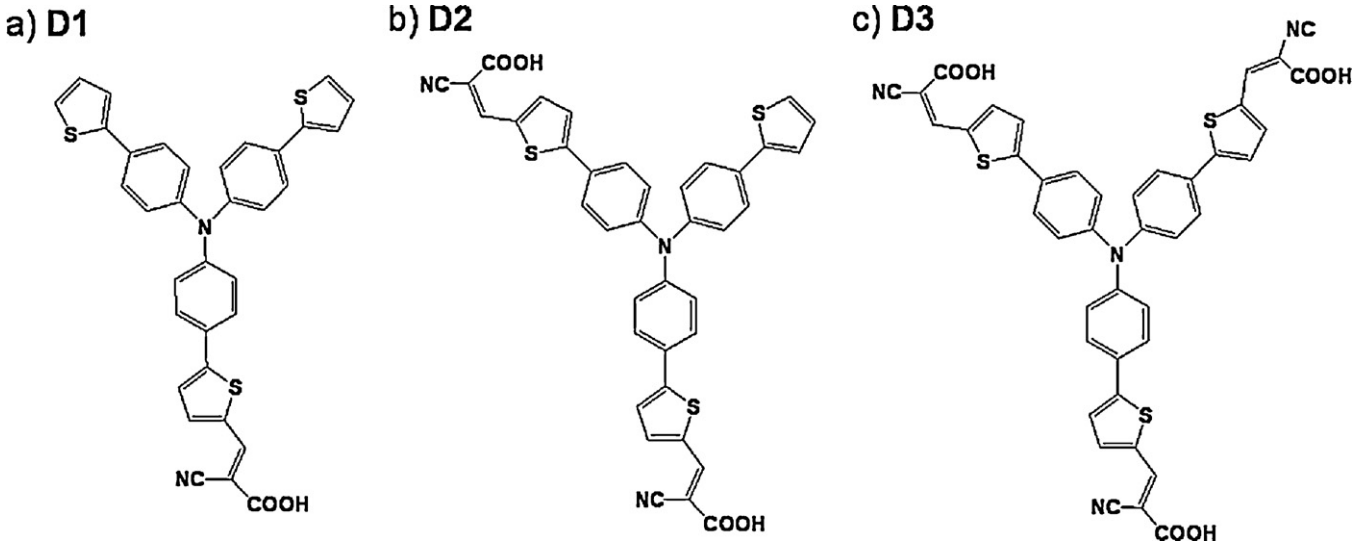

Scheme 2. Structures of organic dyes used in this study.

H_2PtCl_6 (0.5 wt% with respect to TiO_2 mass), which was irradiated with a 250-W Hg lamp for 30 min. The Pt-deposited TiO_2 (Pt/TiO_2) particles were then filtered, washed, and dried at 80 °C. Transmission electron microscopic images of Pt/TiO_2 showed Pt particles with a size range of approximately 3–5 nm dispersed on TiO_2 particles (ca. 30 nm) (Fig. S1 in Supporting Material). For dye-attached TiO_2 samples, TiO_2 or Pt/TiO_2 particles were dispersed at 0.5 g/L in a mixed solution (20 mL) of ethanol: DMF (v/v = 1:1) with different concentrations of dye (100 μM unless otherwise described) for longer than 12 h. This was then filtered, rinsed with acetonitrile, and dried at 80 °C. A UV–vis spectrophotometer (Shimadzu UV-2450) was used to calculate the amounts of adsorbed dyes from the absorbance differences of the main absorption bands between the initial solution and the filtered solution.

The infra-red (IR) spectra of samples were recorded with an FTIR spectrometer (Spectrum GX, PerkinElmer) equipped with an AutoImage microscope and a liquid nitrogen-cooled DTGS detector. Each sample was diluted with KBr powder and referenced against KBr. In order to produce a single spectrum, 32 scans in the wave number range from 4000 cm^{-1} to 400 cm^{-1} at a resolution of 0.25 cm^{-1} were averaged. The absorption spectra of the dye-sensitized TiO_2 powders diluted by $BaSO_4$ were recorded using a UV–vis spectrophotometer with a diffuse reflectance accessory.

2.3. Dye-sensitized photolysis

The visible light activity of dye-sensitized TiO_2 was tested for the production of molecular hydrogen as well as for the remediation of aqueous pollutants. For the H_2 test, the sensitized catalyst was suspended at 0.5 g/L in an aqueous solution of 10 mM triethanolamine (TEOA) or 10 mM ethylenediaminetetraacetic acid (EDTA) as electron donors. The typical solution pH was around 10 and 4.5 due to the presence of TEOA and EDTA, respectively. If necessary, the pH was adjusted by NaOH and HCl. Prior to irradiation, N_2 gas (>99.9%) was purged through the suspension for 30 min to remove dissolved O_2. A 150-W Xenon arc lamp (Ushio 150-MO) equipped with an AM 1.5G filter was used as the light source and a long-wave pass filter (λ > 420 nm) was placed between the lamp and the reactor. The reactor was sealed with ambient air during photolysis and the head-space gas was analyzed with a gas chromatography (GC, ACME 6100) equipped with a Carboxen-1000 column and a thermal conductivity detector (TCD).

For the remediation of aqueous pollutants (4-chlorophenol and Cr(VI)), dye/TiO_2 samples were suspended at 0.5 g/L in aqueous solutions of 4-chlorophenol (4-CP: 80 μM) or Cr(VI) (0.4 mM). These were then stirred for 30 min in the dark to facilitate their equilibrium adsorption on TiO_2. The sample aliquots were intermittently withdrawn during visible light irradiation and filtered through a 0.45-μm PVDF filter (Millipore). The 4-CP concentrations were monitored using high-performance liquid chromatography (HPLC, YL9100), while the concentration of Cr(VI) was analyzed via a colorimetric method that uses 1,5-diphenylcarbazide (DPC) reagent [26]. The color change was monitored at 540 nm ($\varepsilon = 4 \times 10^4$ L mol^{-1} cm^{-1}) using a UV–vis spectrophotometer.

3. Results and discussion

3.1. Spectroscopic analysis of dyes and dye/TiO_2 samples

Fig. 1a shows the UV–vis absorption spectra of free D1, D2, and D3 in a mixed solution of ethanol and DMF. The overall spectra are quite similar in terms of two distinct absorption bands at around 350 and 440 nm. The former arises from π–π* transition, while

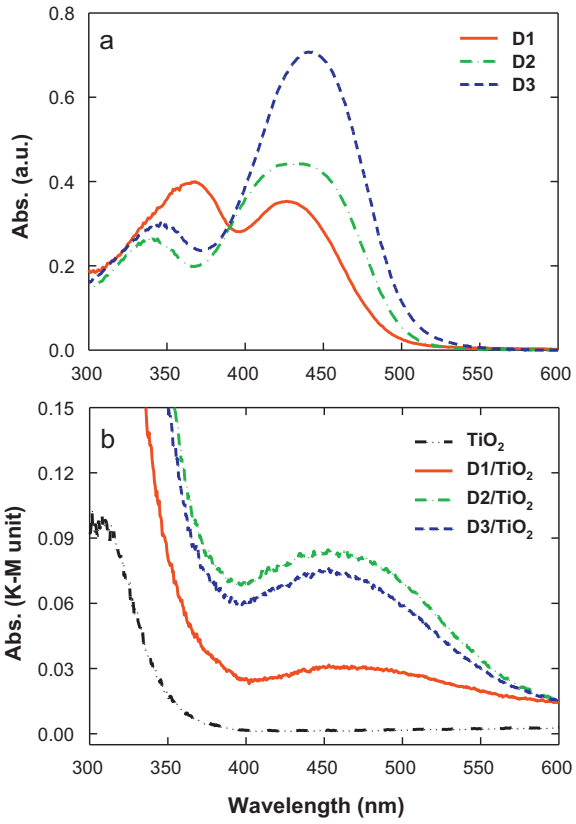

Fig. 1. UV–vis absorption spectra of (a) free dyes (10 μM) and (b) bare TiO_2 and dye/TiO_2 samples. In (b), absorbance was expressed as a Kubelka–Munk unit.

the latter might be attributed to the HOMO–LUMO transition or the intramolecular charge transfer between the donor (D: triphenylamine) and the acceptor (A: 2-cyanoacrylic acid) (Scheme 2) [16–19]. The dyes with more acceptors (D2 and D3) display the red-shifted spectra by approximately 5–10 and 10–20 nm, and exhibit higher molar extinction coefficients by approximately 25 and 200%, respectively, as compared to D1 (Table 1) [25]. Such bathochromic effects of D2 and D3 likely result from the symmetric arrangement of acceptors [21–23,25], while the enhanced absorption property may be due to the greater effect of conjugated π-chromophores. When these dyes are anchored to TiO_2, their intramolecular charge transfer bands are ca. 10–40 nm-red shifted as compared to the respective free dyes (Fig. 1b). These red shifts by adsorption on the TiO_2 surface could be ascribed to the aggregation of dye molecules [15,27]. It should be noted that such intramolecular charge transfer bands play a crucial role in dye-sensitized photocatalysis because the degree of light harvesting takes place most significantly around at the transition bands (Fig. S2). We have found that dyes with higher molar extinction coefficients at the bands could absorb more photons and generate more electrons if other photochemical conditions are identical.

To gain insight on the binding states of dyes, FTIR analyses are performed for free D1, adsorbed D1 (i.e., $D1/TiO_2$) and bare TiO_2 samples (Fig. 2). The major IR bands of free dyes are identified as follows [8,28,29]: 1183 cm^{-1} for C—O—H bending; 1261 cm^{-1} for singly bonded C—O stretching; 1321 cm^{-1} for the symmetric stretching of CO_2^-; 1572 cm^{-1} for the asymmetric stretching of CO_2^-; 1686 and 1696 cm^{-1} for C=O stretching of H-bonded acid; 1716 cm^{-1} for C=O stretching of non H-bonded acid; 2217 cm^{-1} for the stretching of C≡N; 2962 cm^{-1} for the O—H stretching of carboxylic acid. The co-existence of C—O—H-footprinted and

Table 1
Physicochemical properties of organic dyes and dye-sensitized production of molecular hydrogen and remediation of water pollutants.

Dyes	ε_{max} (M^{-1} cm^{-1})[a]	E_{0-0} (eV)[b]	HOMO (V)[c]	LUMO (V)[c,d]	H_2 (μmol)[e]				$k_{4\text{-CP}}$ (min^{-1})[f]	$k_{Cr(VI)}$ (min^{-1})[f]
					TEOA		EDTA			
					P25	HBK	P25	HBK		
D1	35,300	2.55	0.99	−1.56	20.4	59.7	3.5	17.1	0.053	0.029
D2	44,300	2.21	1.15	−1.03	44.7	98.4	4.6	19.4	0.096	0.033
D3	70,700	2.18	1.12	−1.09	40.0	110.5	15.3	21.8	0.060	0.014

[a] Extinction coefficient at maximum absorption of the dyes in DMF/EtOH (1:1) solution.
[b] Determined from the absorption edges of the absorption spectra in a DMF solution.
[c] Obtained as an electron volt (eV) by cyclic voltammetry in DMF and converted into volt vs. NHE.
[d] $E_{HOMO} - E_{0-0} = E_{LUMO}$.
[e] Produced in dye-sensitized Pt/TiO_2 (Degussa P25 and Hombikat UV-100) suspensions after 90 min-irradiation in the presence of 10 mM TEOA (pH 10) or 10 mM EDTA (pH 4.5).
[f] Pseudo-first order kinetics for remediation of 4-chloropenol (4-CP: 80 μM) and Cr(VI) (0.4 mM) in dye-sensitized TiO_2 (P25) suspensions under visible light in the presence of dissolved oxygen.

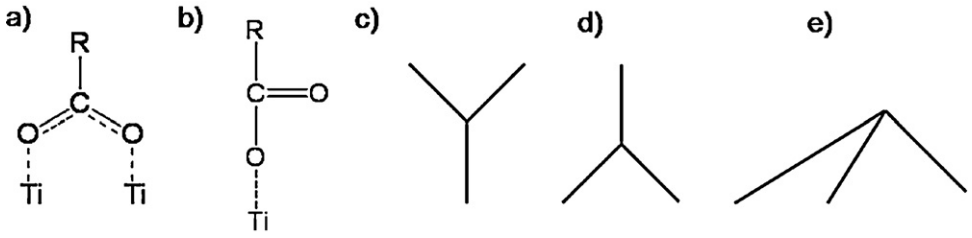

Scheme 3. Structures for possible surface binding states of dyes anchored on TiO_2: (a) bidentate, (b) monodentate, (c) upright Y-type binding (single carboxylate linked), (d) inverted Y-type binding (two carboxylates linked), and (e) tripod binding (three carboxylates linked).

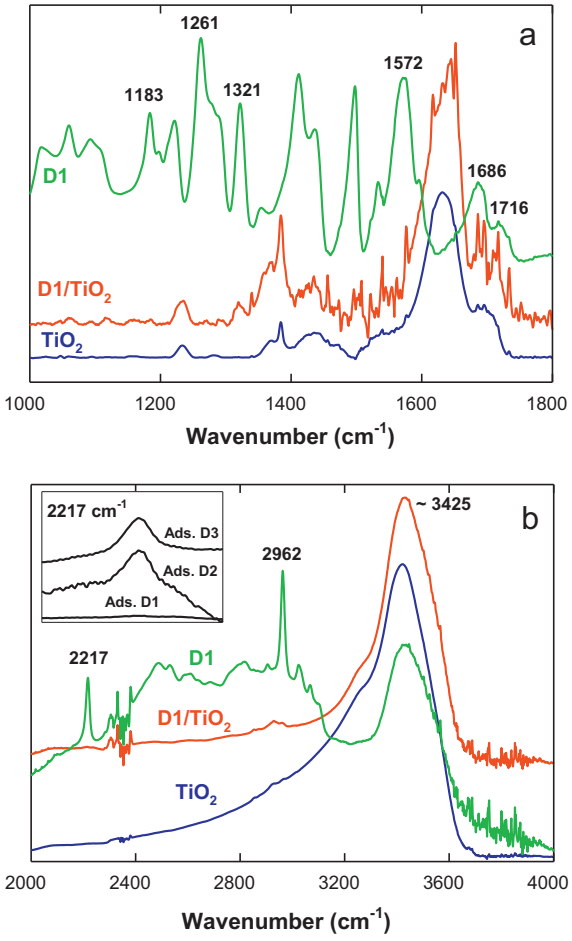

Fig. 2. FTIR spectra of free D1, D1/TiO_2, and bare TiO_2 in (a) low wavenumber and (b) high wavenumber ranges. Inset: FTIR spectra of D1/TiO_2, D2/TiO_2, and D3/TiO_2 samples for bands at 2217 cm^{-1}.

CO_2^--footprinted bands indicates that free D1 possesses both protonated and deprotonated carboxylic groups. When the IR spectrum of D1/TiO_2 is compared to those of free D1 and bare TiO_2, the most prominent changes are seen to be decreases of the band intensities at 1183 cm^{-1} (δ(C—O—H), 1261 cm^{-1} (ν(C—O)), 1321 cm^{-1} ($\nu_s(CO_2^-)$), and 2962 cm^{-1} (ν(O—H)). Such decreases indicate that D1 is attached to TiO_2 through a bindentate coordination (Scheme 3a). However, increase in intensities of the bands at 1686 and 1696 cm^{-1} (ν(C=O) of carboxylic acid) for D1/TiO_2 as compared to that of bare TiO_2 further suggests that a monodentate coordination via hydrogen bonding between —COOH and Ti—OH (3425 cm^{-1}) may exist (Scheme 3b); however the contribution appears to be insignificant.

Overall patterns of IR spectra for D2/TiO_2 and D3/TiO_2 are very similar to that of D1/TiO_2 (Fig. S3), with the one exception being the band at 2217 cm^{-1} (C≡N stretch). As compared in Fig. 2b inset, D2/TiO_2 displays a much stronger C≡N band than D1/TiO_2, a similar band intensity to D3/TiO_2. The trace level of the C≡N band at D1/TiO_2 suggests that when bound to TiO_2 the IR intensity for the nitrile band of 2-cyanoacrylic acid is very weak. Taking this to be true, the stronger nitrile bands of D2/TiO_2 imply that only a single carboxylic acid of D2 is used for the binding and thus the other carboxylic acid remains free (upright Y-type: see Scheme 3c). In addition, the similar intensity of the bands between D2/TiO_2 and D3/TiO_2 further indicates that both dyes possess a similar number of free (unbound) carboxylic acids. As such, the two carboxylic groups of D3 might be used as the anchor (inverted Y-type: Scheme 3d). D2 also can be attached to TiO_2 by using both carboxylic groups; however the chance of success appears to be lower than that of D3. Therefore, D1 can have only the upright Y-type binding mode, while D2 can have either the upright Y-type or the inverted Y-type binding mode, depending on condition. In the case of D3, all three types of binding modes (upright Y, inverted Y, and even tripod) are possible in principle. However, the tripod mode appears to be very unreliable in terms of molecular structure and binding stability.

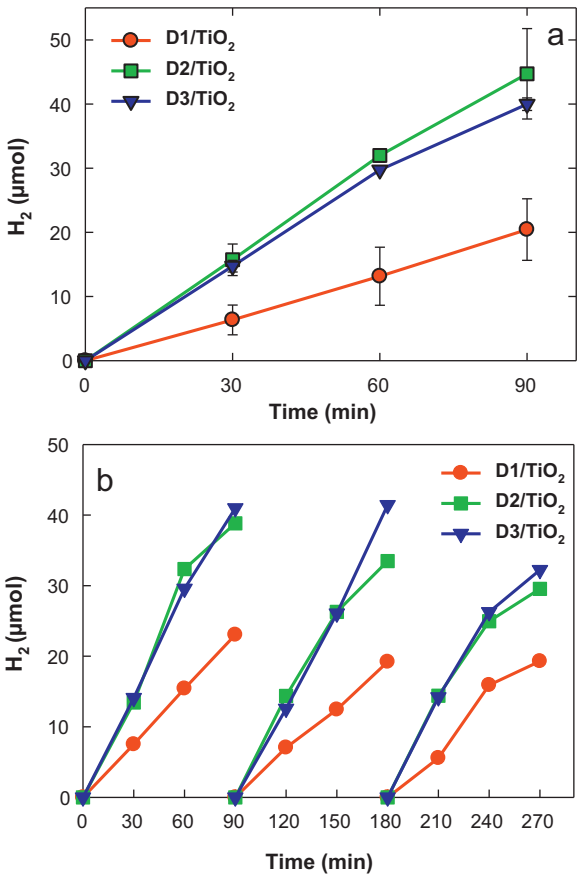

Fig. 3. (a) Time-profiled H_2 productions in dye-sensitized TiO_2 suspensions with TEOA as an electron donor under visible light ($\lambda > 420$ nm). (b) Repeated runs for H_2 production of (a). Here TiO_2 means Pt/TiO_2. [Dye/TiO_2] = 0.5 g/L; $[Dye]_0$ = 100 μM for adsorption; [TEOA] = 10 mM; pH 10; N_2-purged through the suspension for 30 min prior to photolysis.

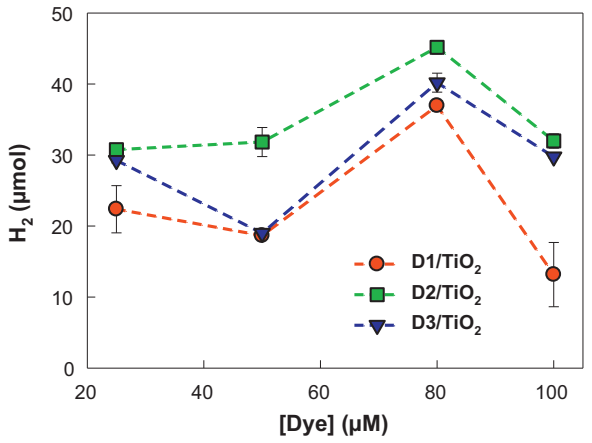

Fig. 4. Effect of initial dye concentrations (25 μM ≤ $[Dye]_0$ ≤ 100 μM) on the sensitized H_2 production. Experimental conditions identical to those of Fig. 3.

3.2. Photocatalytic performances of dye-sensitized TiO_2

3.2.1. Hydrogen production

Fig. 3a shows the time-profiled hydrogen evolution in visible light-irradiated dye/TiO_2 suspensions in the presence of TEOA as an electron donor. It is found that the amount of H_2 evolution is very low in the absence of either Pt deposit or electron donor (data not shown). However, when TiO_2 is platinized (Pt/TiO_2; hereafter, it is referred to as TiO_2 for simplicity) and TEOA is added to the suspension, H_2 is produced rather linearly with irradiation time with the following order of activity: D3–D2 > D1 (Table 1 and Fig. S2). This activity order for the H_2 production appears to be meaningful when a comparison of optical properties is carried out. For example, the ratios of $H_{2,D2}/H_{2,D3}$ (1.12) and $H_{2,D2}/H_{2,D1}$ (2.19) are greater than those of $\varepsilon_{D2}/\varepsilon_{D3}$ (0.62) and $\varepsilon_{D2}/\varepsilon_{D1}$ (1.25), respectively. This suggests that unknown factors affecting the sensitization efficiency exist and that such factors may play a dominant role in D2-sensitization. The activity order is maintained for repeated runs (Fig. 3b); the third run displays a somewhat reduced H_2 production, likely due to consumption of TEOA. This conjecture is reasonable if one electron is transferred from a single TEOA molecule ($[TEOA]_0$ = 10 mM × 0.02 L = 200 μmol), because the total amount of H_2 produced in three runs is approximately 110 μmol, corresponding to 220 μmol-electrons ($2e^-$ per H_2).

The effect of dye concentration on the H_2 production is also studied (Fig. 4). Irrespective of the dye kind, the amount of H_2 increases with increasing dye concentrations of up to [dye] < 80 μM and decreases at [dye] = 100 μM. It is found that all the three dyes can be attached to TiO_2 (Degussa P25) at maximum ~80 μM (i.e., 160 μmol/g-TiO_2). In general, a higher sensitization effect is expected at higher surface concentrations. However, excessive surface concentration of dyes, particularly those with carboxylic acid groups as an anchor, is found to decrease the sensitization effect. This is primarily due to the agglomerating nature of the dyes [7,9]. A similar deactivation appears to occur in D1, D2, and D3 for H_2 evolution. Therefore, employing other TiO_2 samples with larger surface areas may be an alternative method to avoid the deactivation. For example, the commercially available Hombikat TiO_2 (HBK) with a large surface area of ca. 300 m^2/g boosts 2–3-fold larger amounts of H_2 production than P25 TiO_2 with a surface area of ca. 50 m^2/g at [dye] = 100 μM (Table 1).

EDTA is also tested as an electron donor and its effect on the sensitized hydrogen production is compared to that of TEOA (Fig. 5a). The most obvious effect is a substantially reduced amount of H_2 production as compared to the case of TEOA (e.g., $H_{2,EDTA}/H_{2,TEOA}$ for D1, D2, and D3 = 0.17, 0.1, and 0.37, respectively; see Table 1). EDTA has been known to hamper the adsorption of dyes, in particular those with carboxylic acids as the anchoring group, when dyes and EDTA are simultaneously adsorbed onto TiO_2 [7]. In this study, dyes are preadsorbed on TiO_2 in an organic solution and the obtained dye/TiO_2 samples are then used for H_2 production in an aqueous solution. Hence, the competitive adsorption between dye and EDTA is absent; instead it is possible for the preadsorbed dyes to be desorbed from TiO_2 during (or by) photolysis in the presence of EDTA.

It should be noted that the adsorption and desorption of dyes is highly sensitive to pH due to different acid-dissociation behaviors between dyes and TiO_2 (pH_{zpc} ~6.2). In this regard, the H_2 amounts are measured at different pH values and compared with those in the TEOA solution (Fig. 5b). It is apparent that EDTA is more effective at producing H_2 in the acidic pH range, whereas TEOA is more effective in the alkaline pH range. In the case of EDTA, the H_2 amount is largest at pH ~4.5 and decreases thereafter, whereas it increases with increasing pH by way of exponential growth in the presence of TEOA. This pH-dependent H_2 production with EDTA is similar to that exhibited in previous reports [7,10,30], indicating that the adsorption of dyes still plays a key role in sensitization. All the dyes tested for desorption are strongly attached to TiO_2 at pH < ~5 while gradually desorbed from TiO_2 at pH > ~7 (Fig. S4 for D3 desorption). However, we failed to quantify the amounts of the desorbed dye due to the agglomeration of the desorbed dyes and disappearance of the main absorption bands in the aqueous solution (π–π^* transition at ~350 nm and HOMO–LUMO transition at ~450 nm; compare UV–vis spectra in Fig. S4 and Fig. 1). In the case

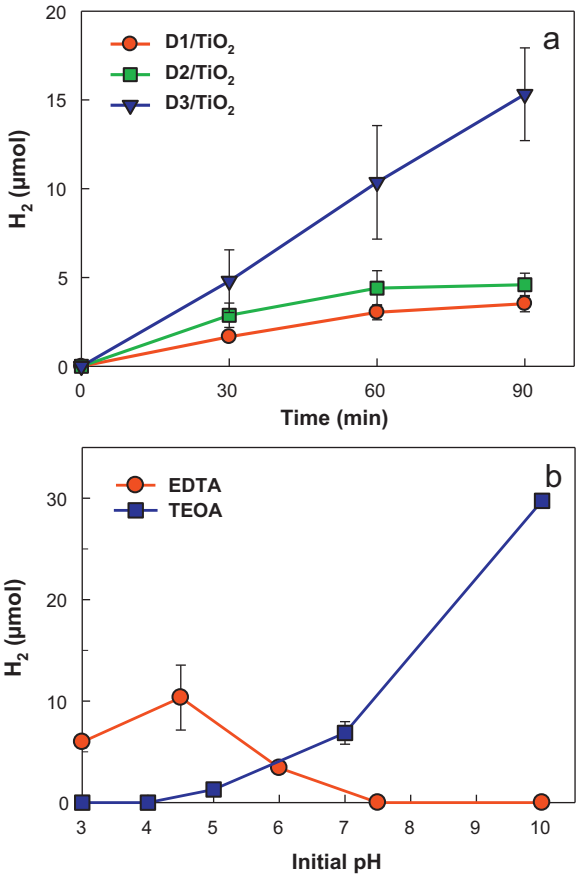

Fig. 5. (a) Time-profiled H_2 productions in dye-sensitized TiO_2 suspensions with EDTA (10 mM; pH 4.5) as an electron donor under visible light ($\lambda > 420$ nm). (b) pH-dependent H_2 production for 1 h in D3-sensitized TiO_2 suspensions under visible light. $[TEOA]_0 = [EDTA]_0 = 10$ mM.

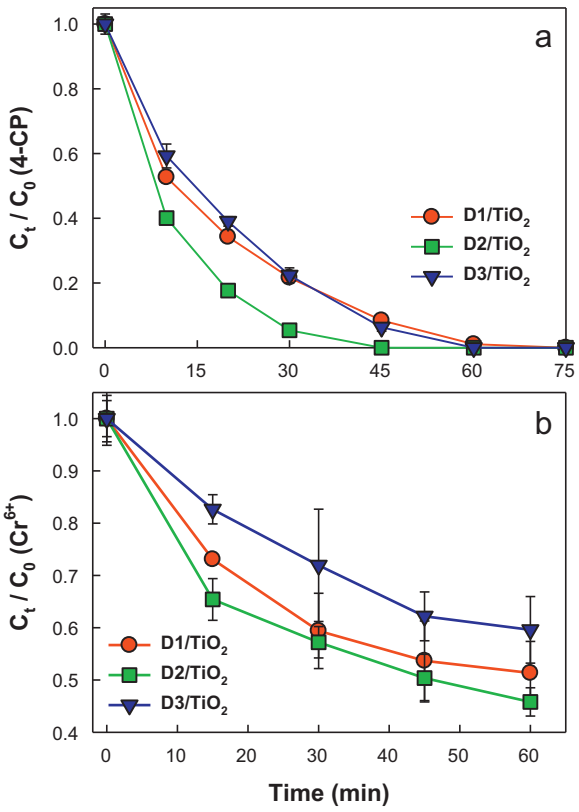

Fig. 6. Decay profiles of (a) 4-chlorophenol (4-CP) and (b) Cr(VI) in visible light-irradiated dye/TiO_2 suspensions. $[Dye/TiO_2] = 0.5$ g/L; $[4\text{-CP}]_0 = 80$ μM; $[Cr(VI)]_0 = 0.4$ mM; open to air.

of TEOA, the pH-dependent H_2 production is also very similar to that exhibited in previous reports. The H_2 amount becomes larger at the alkaline pH values irrespective of sensitizers despite the fact that the sensitization mechanism has not yet been fully disclosed [31–34]. It should be noted that the dye-sensitized TiO_2 electrodes display no measurable dye desorption in severe conditions (1 M HCl and 1 M NaOH) during the photoelectrochemical tests (Fig. S5). In contrast, the dye/TiO_2 suspensions exhibit the pH-dependent desorption of dye during the sensitized hydrogen evolution reaction. The lack of dye desorption of the former could be attributed to the applied electrical potential of dye/TiO_2 electrodes, somehow increasing electrostatic interaction between dye and TiO_2 and thereby enhancing the binding force of the dye.

3.2.2. Environmental remediation

The applicability of sensitized TiO_2 to remediation of aqueous pollutants is also explored. For this exploration, 4-chlorophenol and Cr(VI) are chosen as model substrates and their photo-sensitized remediation is tested. As shown in Fig. 6a, all three organic dyes are found to be very effective in degrading 4-CP under visible light. Kinetic analysis indicates that a pseudo first order decay rate of 4-CP is 0.096 min^{-1} with D2, more than 1.6–1.8 times higher than those of D1 and D3. Decay of 4-CP accompanies the production of chlorides and CO_2 (data not shown), the pattern of which is consistent with literature [11]. These dyes are even active for the remediation of Cr(VI) with the following order: D2 > D1 > D3 (Fig. 6b and Table 1). It should be noted that the remediation mechanisms of 4-CP and Cr(VI) are different to each other, as in the case in H_2 production. The remediation of 4-CP is primarily initiated by a direct electron transfer to the oxidized dye (Dye^+: see reaction 5 and 6 in Scheme 1). The photogenerated electrons from the dye may be quenched by dissolved oxygen at the TiO_2 surface, forming superoxide anion (O_2^-: reaction 8). This is then transformed into hydroperoxy radicals (•OOH) and hydrogen peroxides (H_2O_2) by coupling with protons. These reactive oxygen species may also take part in the 4-CP oxidation. In the case of Cr(VI), the primary remediation mechanism is the conversion of Cr(VI) to Cr(III) by photogenerated electrons (direct reduction: reaction 7) or superoxide anion-mediated conversion (indirect reduction: reaction 9 and 10). For the latter, the formation of a superoxide anion (reaction 8) is a prerequisite. In this regard, the remediation mechanism of aqueous substrates is very complicated, with various reaction pathways as compared to the H_2 production that occurs predominantly in the absence of dissolved oxygen (no generation of the reactive oxygen species). Therefore, the molecular interactions among substrates, dyes, and reactive oxygen species seem to be more important factors than the binding states and configuration of dyes in the H_2 production. Furthermore, the stability of dyes may be decreased in the presence of dissolved oxygen due to possible reactions between dyes and reactive oxygen species. As a result, the reactivity order of the dyes for the aqueous pollutants appears to be different from that of the H_2 production.

3.3. Mechanism of sensitized H_2 production

Among the three dyes, the sensitization activity of D2 for H_2 production is changed most significantly by employing the two different electron donors. The smallest change in D3 activity suggests that the three carboxylic anchoring groups are very effective at tightly holding onto the TiO_2 surface. As briefly discussed above, D3 can have three different binding modes (upright Y-type, inverted

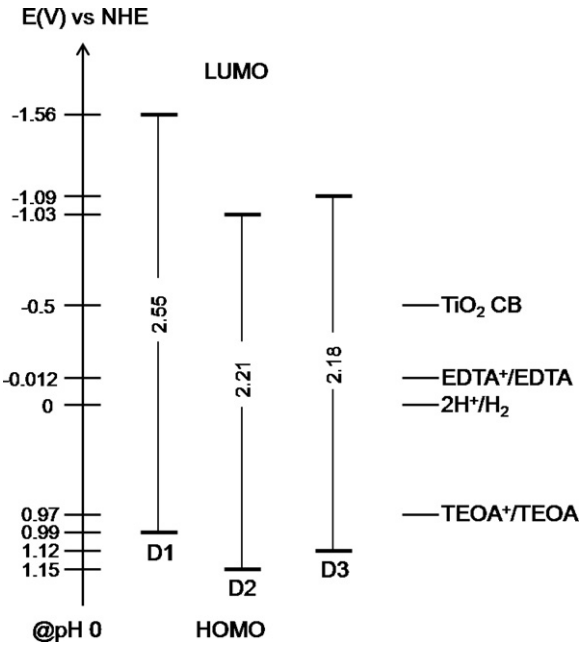

Scheme 4. Diagram for energy levels of components used in this study.

Y-type, and tripod-type: Scheme 3). However, the tripod-type mode may be difficult to maintain in terms of molecular structure and stability. In the case of D1, the upright Y-type mode is only the way to anchor the sensitizer to the TiO_2 surface via a monodentate and/or bidentate adsorption. In contrast, D2 can have either upright Y- or inverted Y-types. When there is an electron donor to be adsorbed onto TiO_2 rather loosely or to have a minor interaction with the TiO_2 surface (e.g., TEOA), D2 can be attached to TiO_2 via the inverted Y-type binding mode. However, in the presence of a strongly competing electron donor (e.g., EDTA), the upright Y-type binding may be favored. In this regard, D2 may have the same binding mode as D3 in the TEOA solution, and with D1 in the EDTA solution. Such a switch in the binding mode of D2 can be indirectly supported by the result that the H_2 amount of D2 is very similar to that of D3 in the TEOA solution, whereas it is similar to that of D1 in the EDTA solution (Fig. 3a vs. Fig. 5a).

This change in the electron donor may also result in the alteration of the relative energy levels that determine the overall charge transfer in H_2 production. Scheme 4 depicts the energy levels of TiO_2, dyes, and electron donors based on the spectroscopic data (Table 1) and literature values. According to this Scheme, all the LUMO levels of dyes are more negative than TiO_2 conduction band while their HOMO levels are more positive than the redox potentials of TEOA and EDTA. Taking into account that the reduction of proton/water on the TiO_2 surface (i.e., Pt/TiO_2) requires an overpotential of around 0.2 V, the overall charge transfers are allowed and consequently the H_2 production is possible. D2 and D3 display similar energy levels, while D1 has the highest (the most negative) HOMO and LUMO levels. Comparison of TEOA and EDTA also suggests that the regeneration of oxidized D2 and D3 is more favored in EDTA due to difference of approximately 1.1 V. It can be deduced that D2 has the most ideal energetics for visible light-sensitization in the presence of TEOA or EDTA. Conversely, the HOMO level of D1 is very close to the one-electron redox potential of TEOA (as compared to that of EDTA). This retards the regeneration of the oxidized D1 by TEOA and consequently increases the recombination between the oxidized D1 and ejected electrons. As such, the recombination may be inhibited with EDTA. Nevertheless, the significantly higher activity for the H_2 production of $D1/TiO_2$ with TEOA than that with EDTA strongly suggests that sensitized H_2 production is very sensitive, not only to the energy levels but also to the electron transfer kinetics that are associated with molecular interaction among dyes, TiO_2 surface, and electron donors.

Finally, it should be noted that in the absence of competitive electron donors the optical property (i.e., absorbance) of dye may be a primary factor determining the sensitization efficiency of dye/TiO_2 system. To examine this conjecture, the photocatalytic H_2 production was monitored in the absence of TEOA and EDTA but no H_2 was detected at all in both cases due to fast recombination of electron–hole pairs. Alternatively, we measured the photocurrents of dye/TiO_2 electrodes in 1 M NaOH electrolyte as a function of irradiation wavelength range and compared their photoconversion performances and UV–vis absorption spectra (Fig. S2). It was found that the photoconversion performances of $D1/TiO_2$, $D2/TiO_2$, and $D3/TiO_2$ display similar fashions to their respective UV–vis absorption spectra. Despite being qualitative, this comparison shows that the optical property of dye also is a very important factor controlling overall photoconversion efficiency in the absence of competitive electron donors.

4. Conclusions

This study demonstrates that Ru-free organic dyes can drive valuable redox reactions by sensitizing TiO_2 particles under visible light. In the sensitization, the number of carboxylate anchoring groups seems to be significantly important because of its effects on the binding states of dyes to TiO_2 as well as on other physicochemical properties such as extinction coefficient and HOMO–LUMO position. In H_2 production, the electron transfers from the photoexcited dyes to TiO_2 and from the electron donors to the oxidized dyes appear to be the primary reactions that determine overall performance. As such, the dye structure becomes relatively important. The H_2 experiment further indicates that use of dyes with multi-anchoring groups is more desirable than those with a single anchoring group. Meanwhile, the remediation of aqueous pollutants involves not only the electron transfers but also the redox reactions of pollutants on the TiO_2 surface through direct and dissolved oxygen-mediated electron transfers. As a result, the dye structure becomes less important as compared to the H_2 production. This result suggests that the optimal dye structure varies depending on the purpose and application, and thus more diverse organic dyes should be prepared and tested to gain a deeper insight on the effect of dye structures.

Acknowledgement

This research was supported by the Basic Science Research Programs (Nos. 2009-0071350, 2009-0089904, 2010-0002674, and 2011-0021148) and by the Korea Center for Artificial Photosynthesis (NRF-2011-C1AAA001-2011-0030278) through the National Research Foundation of Korea (NRF) funded by the Ministry of Education, Science and Technology.

Appendix A. Supplementary data

Supplementary data associated with this article can be found, in the online version, at http://dx.doi.org/10.1016/j.apcatb.2012.04.011.

References

[1] B. O'Regan, M. Gratzel, Nature 353 (1991) 737.
[2] A.J. Bard, M. Stratmann (Eds.), Semiconductor Electrodes and Photoelectrochemistry, Wiley-VCH, 2002.
[3] C.A. Grimes, O.K. Varghese, S. Ranjan (Eds.), Light, Water, Hydrogen, Springer, New York, 2008.

[4] K. Maeda, K. Teramura, D. Lu, T. Takata, N. Saito, Y. Inoue, K. Domen, Nature 440 (2006) 295.
[5] W.J. Youngblood, S.-H.A. Lee, Y. Kobayashi, E.A. Hernandez-Pagan, P.G. Hoertz, T.A. Moore, A.L. Moore, D. Gust, T.E. Mallouk, J. Am. Chem. Soc. 131 (2009) 926–927.
[6] E. Bae, W. Choi, Environ. Sci. Technol. 37 (2003) 147–152.
[7] E. Bae, W. Choi, J. Phys. Chem. B 110 (2006) 14792–14799.
[8] E. Bae, W. Choi, J.W. Park, H.S. Shin, S.B. Kim, J.S. Lee, J. Phys. Chem. B 108 (2004) 14093–14101.
[9] H. Park, E. Bae, J.J. Lee, J. Park, W. Choi, J. Phys. Chem. B 110 (2006) 8740–8749.
[10] H. Park, W. Choi, Langmuir 22 (2006) 2906–2911.
[11] Y. Park, S.H. Lee, S.O. Kang, W. Choi, Chem. Commun. 46 (2010) 2477–2479.
[12] K.S. Finnie, J.R. Bartlett, J.L. Woolfrey, Langmuir 14 (1998) 2744–2749.
[13] A. Fillinger, D. Soltz, B.A. Parkinson, J. Electrochem. Soc. 149 (2002) A1146.
[14] M.K. Nazeeruddin, R. Humphry-Baker, P. Liska, M. Graetzel, J. Phys. Chem. B 107 (2003) 8981.
[15] K. Hara, Z.S. Wang, T. Sato, A. Furube, R. Katoh, H. Sugihara, Y. Dan-oh, C. Kasada, A. Shinpo, S. Suga, J. Phys. Chem. B 109 (2005) 15476–15482.
[16] K.R.J. Thomas, Y.C. Hsu, J.T. Lin, K.M. Lee, K.C. Ho, C.H. Lai, Y.M. Cheng, P.T. Chou, Chem. Mater. 20 (2008) 1830–1840.
[17] J. Wiberg, T. Marinado, D.P. Hagberg, L.C. Sun, A. Hagfeldt, B. Albinsson, J. Phys. Chem. C 113 (2009) 3881–3886.
[18] J.H. Yum, D.P. Hagberg, S.J. Moon, K.M. Karlsson, T. Marinado, L.C. Sun, A. Hagfeldt, M.K. Nazeeruddin, M. Gratzel, Angew. Chem.-Int. Edit. 48 (2009) 1576–1580.
[19] A. Abbotto, N. Manfredi, C. Marinzi, F. De Angelis, E. Mosconi, J.H. Yum, X.X. Zhang, M.K. Nazeeruddin, M. Gratzel, Energy Environ. Sci. 2 (2009) 1094–1101.
[20] J.H. Kim, K.S. Ahn, Jpn. J. Appl. Phys. 49 (2010) 060219.
[21] Y.S. Yang, H. Do Kim, J.H. Ryu, K.K. Kim, S.S. Park, K.S. Ahn, J.H. Kim, Synth. Met. 161 (2011) 850–855.
[22] J. Xu, L. Wang, G.J. Liang, Z.K. Bai, L.X. Wang, W.L. Xu, X.L. Shen, Spectroc. Acta Pt. A-Molec. Biomolec. Spectr. 78 (2011) 287–293.
[23] F. Zhang, Y.H. Luo, J.S. Song, X.Z. Guo, W.L. Liu, C.P. Ma, Y. Huang, M.F. Ge, Z.S. Bo, Q.B. Meng, Dyes Pigm. 81 (2009) 224–230.
[24] W. Kim, T. Tachikwawa, T. Majima, C. Li, H.-J. Kim, W. Choi, Energy Environ. Sci. 3 (2010) 1789–1795.
[25] Y.S. Yang, H.S. Yang, J.-H. Ryu, K.K. Kim, K.-S. Ahn, J.-H. Kim, submitted for publication (2011).
[26] L.S. Clesceri, A.E. Greenberg, A.D. Eaton, Standard Methods for the Examination of Water and Wastewater, APHA, AWWA, WEF, Washington, DC, 1998.
[27] T. Kitamura, M. Ikeda, K. Shigaki, T. Inoue, N.A. Anderson, X. Ai, T. Lian, S. Yanagida, Chem. Mater. 16 (2004) 1806–1812.
[28] M.K. Nazeeruddin, M. Amirnasr, P. Comte, J.R. Mackay, A.J. McQuillan, R. Houriet, M. Gratzel, Langmuir 16 (2000) 8525–8528.
[29] P. Qu, D.W. Thompson, G.J. Meyer, Langmuir 16 (2000) 4662–4671.
[30] D.N. Furlong, D. Wells, W.H.F. Sasse, J. Phys. Chem. 90 (1986) 1107–1115.
[31] S.K. Choi, S. Kim, J. Ryu, S.K. Lim, H. Park, submitted for publication (2011).
[32] R. Abe, K. Hara, K. Sayama, K. Domen, H. Arakawa, J. Photochem. Photobiol. A 137 (2000) 63–69.
[33] Y.X. Li, C.F. Xie, S.Q. Peng, G.W. Lu, S.B. Li, J. Mol. Catal. A 282 (2008) 117–123.
[34] T. Puangpetch, P. Sommakettarin, S. Chavadej, T. Sreethawong, Int. J. Hydrogen Energy 35 (2010) 12428–12442.